Journal of proteome research

Article

Cite This: J. Proteome Res. 2018, 17, 479−485

pubs.acs.org/jpr

# Proteomic Characterization of Dermal Interstitial Fluid Extracted Using a Novel Microneedle-Assisted Technique

Bao Quoc Tran,[†,⊥] Philip R. Miller,[‡,⊥] Robert M. Taylor,[§] Gabrielle Boyd,[†] Phillip M. Mach,[†] C. Nicole Rosenzweig,[∥] Justin T. Baca,[§] Ronen Polsky,[*,‡] and Trevor Glaros[*,∥]

[†]Excet, Inc., 6225 Brandon Avenue, Suite 360, Springfield, Virginia 22150, United States

[‡]Sandia National Laboratories, Albuquerque, New Mexico 87185, United States

[§]Department of Emergency Medicine, The University of New Mexico, Albuquerque, New Mexico 87131, United States

[∥]Research and Technology Directorate, US Army Edgewood Chemical Biological Center, Aberdeen Proving Ground, Maryland 21010, United States

Supporting Information

**ABSTRACT:** As wearable fitness devices have gained commercial acceptance, interest in real-time monitoring of an individual's physiological status using noninvasive techniques has grown. Microneedles have been proposed as a minimally invasive technique for sampling the dermal interstitial fluid (ISF) for clinical monitoring and diagnosis, but little is known about its composition. In this study, a novel microneedle array was used to collect dermal ISF from three healthy human donors and compared with matching serum and plasma samples. Using a shotgun quantitative proteomic approach, 407 proteins were quantified with at least one unique peptide, and of those, 135 proteins were differently expressed at least 2-fold. Collectively, these proteins tended to originate from the cytoplasm, membrane bound vesicles, and extracellular vesicular exosomes. Proteomic analysis confirmed previously published work that indicates that ISF is highly similar to both plasma and serum. In this study, less than one percent of proteins were uniquely identified in ISF. Taken together, ISF could serve as a minimally invasive alternative for blood-derived fluids with potential for real-time monitoring applications.

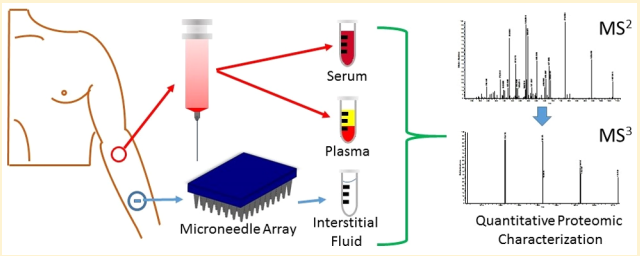


**KEYWORDS:** *proteomics, interstitial fluid, wearable sensing, blister fluid, microneedles*

## INTRODUCTION

Skin is the largest and most often overlooked organ in the human body. This organ's primary function is to protect the underlying tissue from external insults, but it is also responsible for sensing the surrounding environment. Skin is composed of three main layers (outermost to innermost): the epidermis, the dermis, and the hypodermis. The stratum corneum, primarily composed of corneocytes, is the outermost layer of the epidermis and is predominately responsible for providing a hydrophobic barrier to the environment and to potential pathogens. Between the epidermis and the dermis is a region known as the basement membrane. This region is composed of a thin layer of extracellular matrix that connects the two layers, providing a space for cell trafficking and a reservoir of molecules required for a variety of biological purposes including wound repair and immunity. Vascular and nerve structures are found largely in the hypodermis and deeper layers of the dermis.

Presently, other than for diagnosing cancer,[1] glucose testing in subjects with diabetes,[2−4] or testing for cystic fibrosis,[5] skin is not routinely used for clinical laboratory testing. Traditional biofluids such as blood and urine are most commonly used for diagnostic testing. However, with the growing need for noninvasive sampling and real-time physiological monitoring, interest in exploring the skin as a reservoir of information has grown in recent years.[6−8] Sampling near the basement membrane space between the epidermis and the dermis or in the less vascularized regions of the papillary dermis can provide interstitial fluid as a potential alternative to blood, but there is a paucity of knowledge on the presence of useful physiological markers.

Microneedles have recently been proposed as a new sample collection method for clinical diagnosis.[9−13] The advantage of microneedles versus traditional hypodermic needles is that they do not reach nerve endings or vasculature within the dermis and are therefore painless and minimally invasive. Instead of sampling blood, microneedles sample the extracellular fluid within the dermis or between the epidermis and dermis. Interstitial fluid is thought to be composed primarily of blood components due to exchange that takes place between the interstitium and local vasculature.[14] Performing proteomics on plasma and serum is of clinical importance and is particularly challenging due to the large dynamic range of proteins within

**Received:** September 7, 2017
**Published:** November 24, 2017





DOI: 10.1021/acs.jproteome.7b00642
J. Proteome Res. 2018, 17, 479−485

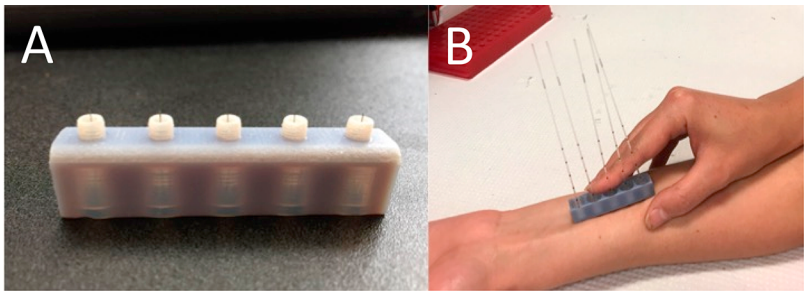


**Figure 1.** Microneedle Device. (A) An array of five ultrafine nano pen needles were assembled within a 3D printed holder. (B) The device was placed on the forearm of each donor and microcapillaries were attached to each needle to collect interstitial fluid.

the blood.[15] Unfortunately, many of the biomarkers are at relatively low levels, and their detection is problematic due to the highly abundant proteins such as serum albumin. Many strategies have been employed to overcome this problem including both affinity depletion and extensive sample fractionation strategies. In fact, a recent report used both strategies as part of a quantitative proteomics pipeline to characterize suction blister fluid (SBF) from eight healthy donors.[16] This work established that the protein content of SBF was highly similar to blood plasma due to the fact that the highly abundant proteins between the two fluid types were conserved. Detailed understanding of the protein content of pure dermal interstitial fluid is an essential step to fully understanding its diagnostic potential.

Using a simply constructed microneedle array with no suction apparatus, ISF was collected from three healthy human donors along with matching serum and plasma. Because the volumes of ISF were relatively small (<20uL), a fractionation-only, quantitative proteomics pipeline was employed to critically characterize ISF's protein content compared with both serum and plasma. This work revealed that the three fluids were incredibly similar, especially in total protein diversity. Given the simplicity of this new method and the similarity of ISF to both plasma and serum, this work suggests that ISF may serve as a viable minimally invasive fluid for clinical applications including the novel application of wearable real-time sensing devices.

## EXPERIMENTAL SECTION

### Microneedle-Assisted Extraction of ISF

The University of New Mexico Human Research Review Committee approved all experiments involving human subjects, and informed consent was documented prior to participation. Subjects were 18 years of age or older, had no known skin disease, and were not taking anticoagulant medications. Subjects with a known allergy to medical tape were also excluded. Arrays of 32 G Ultrafine Nano pen needles (BD, Franklin Lakes, NJ) were constructed using a 3D-printed holder. The device was developed at Sandia National Laboratory (Polsky et al.) and the University of New Mexico (Baca et al.) (manuscript in preparation). The 3D-printed microneedle-array holders (Figure 1) were sterilized prior to use, and skin was cleansed with isopropyl alcohol swab prior to array application. The microneedle array was gently pressed against subject's forearm while in a seated posture and held in place either manually or with 1 in. Coban, latex-free, self-adhesive wrap (3 M Health Care, Neuss, Germany) for the duration of sample collection. Extracted ISF was transferred to microcentrifuge tubes and flash-frozen using liquid nitrogen and stored at −80 °C for later analysis. After completion of sample collection, the forearm of each subject was inspected to make sure that no microneedle was retained in the skin and the skin was again cleansed with an alcohol swab.

### Blood Collection and Separation

Venipuncture was performed prior to microneedle insertions using standard clinical procedures. Blood was preserved in serum separator, sodium fluoride, or sodium EDTA vacutainer collection tubes (BD, Franklin Lakes, NJ) and centrifuged at 3000*g* for 15 min. Serum and plasma fractions were removed and placed in individual microcentrifuge tubes. Serum and plasma samples were flash-frozen using liquid nitrogen and stored at −80 °C until analysis.

### Sample Preparation for Proteomic Analysis of ISF, Plasma, and Serum

The ISF, plasma, and serum samples described above were subjected to tryptic digestion, tandem-mass-tagged (TMT) labeling, and 2D separation prior to mass-spectrometry acquisition. Protein concentration was estimated using Pierce BCA protein assay kit following manufacturer's protocol. An aliquot of ∼135 μg of total protein from each sample was diluted in 200 μL of 50 mM triethylammonium bicarbonate (TEAB) (Sigma-Aldrich, prod no. T-7408) and denatured by adding 300 μL of 10 M urea buffer. Protein reduction was performed by adding 10 μL of 1 M dithiothreitol (Sigma-Aldrich, prod no. D0632-25G) prepared in HPLC-grade water to each sample for a 30 min incubation at 56 °C on a shaker at 400 rpm. Carbamidomethylation of cysteine was carried out with the addition of 40 μL of 0.5 M iodoacetamide (Sigma-Aldrich, St. Louis, MO; cat no. I1149-25G) for 30 min in the dark at room temperature. The alkylated samples were diluted with 1000 μL of 50 mM TEAB solution to a final urea concentration of 2 M prior to overnight tryptic digestion at protease−substrate ratio of 1:50 by adding 4 μg Lys-C/Trypsin (Promega, prod no. V5071) at 37 °C on shaker at 400 rpm. Tryptic digests were acidified with 15 μL of 100% formic acid and cleaned up on 1 $cm^3$ Oasis HLB C18 SPE cartridges (Waters, WAT094225) following manufacturer's protocol. Peptide eluents were vacuum-lyophilized to dryness. Sample was then resuspended in 112.5 μL of 10% acetonitrile/0.1 M TEAB, and an aliquot of 56 μL (33.75 μg) of each sample was taken for isobaric labeling reaction with 10-plex TMT reagents (Thermo Fisher Scientific, Waltham, MA; cat no. 90110) following manufacturer's protocol. The labeled samples were pooled together and lyophilized to dryness.

### Basic Reverse-Phase Peptide Fractionation

First-dimensional fractionation was carried out under basic conditions as previously described.[17] In brief, the pooled


DOI: 10.1021/acs.jproteome.7b00642
J. Proteome Res. 2018, 17, 479−485

peptides were resuspended in 1.5 mL of basic reverse-phase mobile phase A of 10% acetonitrile/100 mM ammonium formate pH 10 and loaded onto a C18 trap column at flow rate of 0.2 mL/min. Peptides were separated at flow rate of 0.5 mL/min on a 4.6 mm × 250 mm, 5 μm XBridge column (Waters) using a gradient profile of 0−5 min: 0% B, 5−13 min: 0 to 15% B, 13−46 min: 15 to 28.5% B, 46−51.5 min: 28.5 to 34% B, and 51.5−64.5 min: 34 to 60% B. Eluent was collected in 4 "beginning" fractions of 2 min, then 84 fractions of 0.5 min that were concatenated in 28 fractions, and 5 "end" fractions of 2 min.[18] Both the beginning and end fractions were pooled into two separate fractions, making for a total of 30 fractions to be analyzed. Each fraction was lyophilized to dryness and stored at −80C.

### Liquid Chromatography Mass Spectrometry Analysis (LC−MS/MS)

Immediately prior to analysis, the fractions were resuspended in 20 μL of acetonitrile/water/formic acid 5/95/0.5 (v/v/v). Two microliters of each fraction was analyzed in a nanoLC system (Dionex, Ultimate 3000) coupled to an Orbitrap Fusion mass spectrometer (Thermo Fisher Scientific, Waltham, MA). Peptides were trapped on a PepMap 300 μm × 5 mm C18, 100A (Thermo Fisher Scientific, Waltham, MA) at flow rate of 10 μL/min for 5 min. Peptide separation was performed on an EASYspray C18 75 μm × 50 cm column over a 182 min gradient at flow rate of 200 nL/min using mobile phase A of 0.1% formic acid in water and mobile phase B of acetonitrile/water/formic acid 80/20/0.1 (v/v/v). LC gradient was 0−150 min: 6−35% B, 150−158 min: 35−60% B, 158−161 min: 60−90% B, 161−171 min: 90% B hold, 171−172 min: 90−6% B, and 172−182 min: 6% B hold.

Mass spectrometric data were acquired using a data-dependent method with time cycles of 3 s. Full MS scans were collected at resolving power of 120 000 over an $m/z$ range 350−1500. The monoisotopic peaks of most abundant peptides detected with charge states 2−7 were isolated for collision-induced dissociation (CID) at normalized collision energy of 35. Fragment ions were measured in the iontrap at turbo scan speed. The top 10 peaks of the MS2 spectrum were then isolated and fragmented using multinotch isolation window of 2 $m/z$ and higher energy collision dissociation (HCD) at a collision energy of 65. HCD MS3 spectra were acquired in orbitrap cell at resolving power 60 000 in an $m/z$ range 120−500. Dynamic exclusion time window of 70 s was set to filter the acquired precursor ions.

### Data Processing and Bioinformatics Analysis

MS data were searched against a UniprotKB *Homo sapiens* database using software Proteome Discoverer 2.1 SP1 (Thermo Fisher Scientific, Waltham, MA). Searching parameters included a precursor mass tolerance of 10 ppm, fragment tolerance of 0.6 Da, maximum missed cleavage level of 2, minimum peptide length of 6, variable modifications of oxidized methionine [+15.99 Da], and acetylated N-protein terminus [+42.011 Da], and static modifications were set to carbamidomethylation of cysteine [+57.02 Da], N-terminal TMT 6 plex [+229.16 Da], and TMT labeling of lysine [+229.16 Da]. Peptide spectrum matches (PSMs) were validated based on $q$ value (FDR = 0.01) using Percolator algorithm,[19] and only the high-confidence PSMs were applied to peptide identification. Peptide identification and protein identification were statistically filtered at high confidence level at a false discovery rate of 1%. A protein identification is determined when it has at least two corresponding peptides identified and one peptide unique to the group of that protein.

Only MS2 spectra above coisolation interference threshold of 50 and MS3 average reporter signal-to-noise threshold of 10 were considered for quantification. To be qualified for quantitation, an identified protein must have at least one identified peptide unique to the protein, and only unique/razor peptides were counted for protein quantitation. Reporter ion intensities (RIIs) were extracted from MS3 spectra at mass tolerance of 20 ppm and normalized to total ion current (TIC) and scaled to 100 for calculating protein relative abundance ratios. The normalized RIIs of proteins were also imported to Perseus 1.5.5.3[20] for statistical analysis of protein abundances among the experimental samples. Annotation enrichment analysis were performed using DAVID 6.8.[21]

## RESULTS AND DISCUSSION

### Dermal Interstitial Fluid Compared to Suction Blister Fluid

In our work, without sample depletion, we identified over three thousand proteins adequate enough for an in-depth comparison

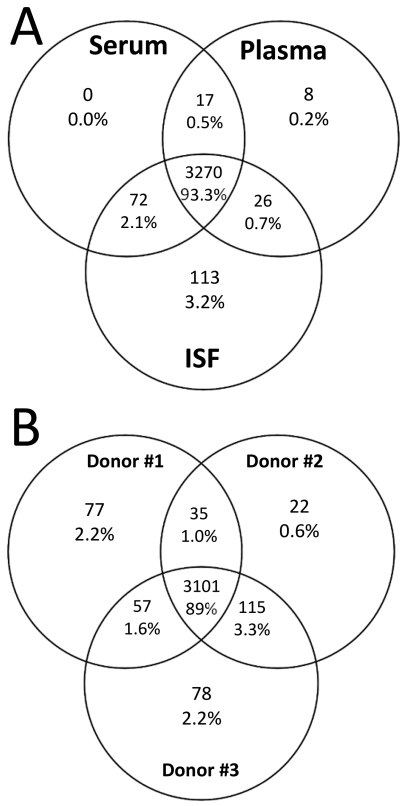


**Figure 2.** Venn diagrams demonstrating distribution of (A) 3506 proteins identified in plasma, serum, and ISF of donor #1, in which 3270 proteins are in common. (B) Complete proteome distribution of the ISF proteins found in common in donors 1, 2, and 3. Overall, 89% of the proteins were consistently detected in all three examined human individuals.

of ISF to plasma and serum (data shown in section below). We found only a couple dozen (<1%) proteins (primarily tubulins) unique to ISF compared with plasma and serum, which contrasted with the protein diversity of SBF detailed in a study performed by Kool et al.[22] The difference in terms of protein composition between ISF and SBF might be caused by the suction used during the sampling technique. Whereas the SBF



DOI: 10.1021/acs.jproteome.7b00642
J. Proteome Res. 2018, 17, 479−485

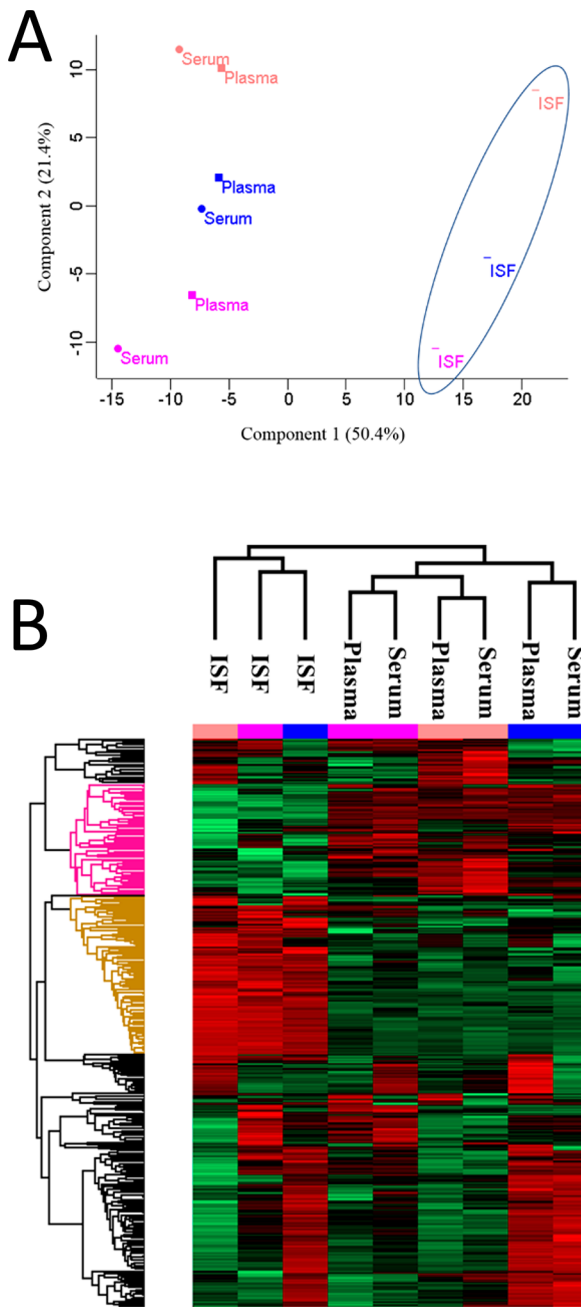


**Figure 3.** Global proteome comparison of ISF to serum and plasma. (A) Principal component analysis of intensities of 407 unambiguously identified proteins that were qualified for quantification. It revealed that ISF samples distinguishably differed from the plasma and serum. (B) Hierarchical clustering analysis demonstrating protein expression profile in ISF, plasma, and serum. Lower expression is shown in green and higher expression is in red.

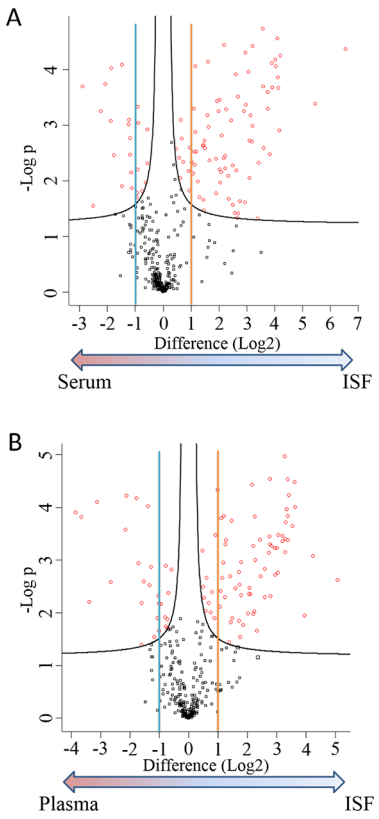


**Figure 4.** Volcano plots demonstrating protein expression of ISF versus serum (A) and ISF versus plasma (B), respectively. 407 quantified proteins from the samples were subject to two-side *t* test with FDR = 0.05 and S0 = 0.1. Red dots represent proteins that were significantly different in abundance between the types of samples. Vertical bars are set for two-fold change in protein expression. Identifications and quantitation ratios of the proteins are shown in Tables S-1 and S-2.

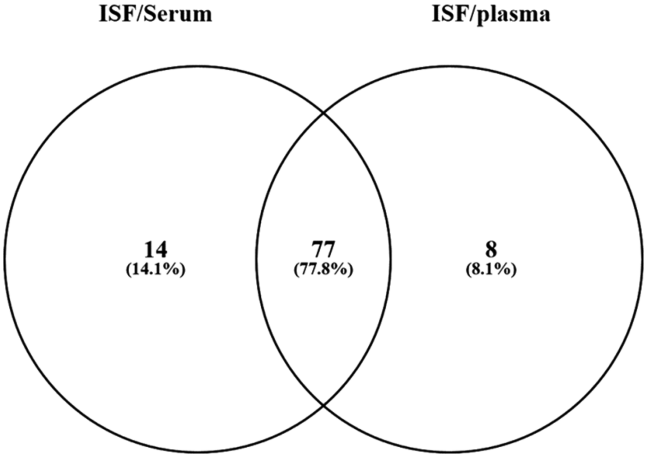


**Figure 5.** Venn diagram comparing proteins found to be enriched ±2-fold in ISF versus serum or plasma.

was collected from a blister forcibly generated under vacuum suction, our microneedle-based ISF was collected passively with minimal tissue damage. Kool et al. showed that when total protein content was normalized prior to analysis, the top 10–20 most abundant proteins remained unchanged.[22] Like SBF, microneedle-derived ISF also showed that some of the most abundant proteins remained unchanged (transferrin and IgGs). However, unlike SBF, many of the top proteins were found to differ in abundance. For example, albumin and alpha-1-antitrypsin were found to be 40–60% higher in ISF compared with both serum and plasma, but complement (C3, C4B, and 4A), apolipoprotein (B, B-100, and A), and haptoglobin were found to be higher in both serum and plasma compared with ISF. Additionally, other work performed on SBF showed that the protein content was significantly different than serum. In fact, Kool et al. showed that SBF was roughly 50% more diverse in its 401 overall proteins compared with serum.[22] The authors



DOI: 10.1021/acs.jproteome.7b00642
*J. Proteome Res.* 2018, 17, 479–485

**Table 1. ANOVA Comparison of ISF to Serum/Plasma for All Donors**

| protein description | accession | ISF/serum donor #1 | ISF/plasma donor #1 | ISF/serum donor #2 | ISF/plasma donor #2 | ISF/serum donor #3 | ISF/plasma donor #3 |
|---|---|---|---|---|---|---|---|
| carbonyl reductase [NADPH] 1 | P16152 | 21.7 | 15.6 | 22.2 | 12.5 | 13.0 | 9.7 |
| creatine kinase B-type | P12277 | 12.2 | 9.7 | 24.4 | 15.6 | 14.9 | 12.0 |
| protein S100-A4 | P26447 | 11.1 | 5.7 | 27.0 | 14.1 | 17.2 | 11.5 |
| alcohol dehydrogenase [NADP+] | P14550 | 13.7 | 13.3 | 23.3 | 13.2 | 13.7 | 9.1 |
| serine protease inhibitor Kazal-type 5 | Q9NQ38 | 13.9 | 10.8 | 24.4 | 14.3 | 14.7 | 8.1 |
| ribonuclease inhibitor | P13489 | 17.9 | 8.9 | 20.0 | 12.2 | 15.2 | 10.6 |
| phosphatidylethanolamine-binding protein 1 | D9IAI1 | 19.2 | 11.8 | 14.9 | 11.0 | 11.2 | 8.8 |
| ubiquitin-like modifier-activating enzyme 1 | P22314 | 14.9 | 7.8 | 18.9 | 11.9 | 12.2 | 11.1 |
| uncharacterized protein | E9PBV3 | 12.7 | 6.2 | 21.3 | 16.1 | 9.0 | 7.9 |
| 72 kDa type IV collagenase | P08253 | 10.0 | 9.8 | 14.9 | 13.3 | 11.2 | 7.6 |
| Sushi, von Willebrand factor type A, EGF and pentraxin domain-containing protein 1 | Q4LDE5 | 10.4 | 8.3 | 10.0 | 8.1 | 16.7 | 11.6 |
| metalloproteinase inhibitor 2 | P16035 | 8.5 | 7.4 | 10.1 | 7.6 | 9.1 | 5.3 |
| neuroblast differentiation-associated protein AHNAK | Q09666 | 6.5 | 5.2 | 11.0 | 11.2 | 6.7 | 6.3 |
| insulin-like growth factor-binding protein 6 | P24592 | 7.0 | 7.2 | 10.2 | 8.0 | 6.5 | 5.5 |
| laminin subunit gamma-1 | P11047 | 5.0 | 5.9 | 5.3 | 4.5 | 8.5 | 5.9 |
| immunoglobulin superfamily containing leucine-rich repeat protein | O14498 | 4.9 | 3.9 | 7.1 | 5.7 | 7.6 | 5.1 |
| cystatin-C | P01034 | 3.5 | 3.3 | 5.7 | 6.2 | 5.5 | 4.7 |
| basement membrane-specific heparan sulfate proteoglycan core protein | P98160 | 3.9 | 4.3 | 5.1 | 5.3 | 4.8 | 4.0 |
| moesin | P26038 | 3.7 | 3.6 | 4.5 | 5.0 | 4.0 | 6.0 |
| gelsolin | P06396 | 3.1 | 2.9 | 3.5 | 3.2 | 2.6 | 2.3 |
| vasorin | Q6EMK4 | 2.0 | 1.9 | 2.5 | 2.5 | 2.0 | 2.2 |
| cDNA FLJ56822, highly similar to alpha-2-HS-glycoprotein | B7Z556 | 1.5 | 1.9 | 1.7 | 2.2 | 1.5 | 2.0 |
| apolipoprotein C−IV | P55056 | 0.4 | 0.3 | 0.4 | 0.4 | 0.3 | 0.4 |
| serpin A11 | Q86U17 | 0.3 | 0.3 | 0.3 | 0.3 | 0.3 | 0.3 |
| coagulation factor V | P12259 | 0.3 | 0.2 | 0.2 | 0.2 | 0.2 | 0.2 |
| von Willebrand factor | P04275 | 0.2 | 0.1 | 0.1 | 0.1 | 0.1 | 0.1 |

attributed this to dynamic range issues with the serum compared with the ISF fluid, even though a depletion technique was used to minimize this problem. As can be seen from this data, proteomic characterization of body fluids is extremely challenging due to its high complexity and the enormous dynamic range of protein concentrations which spans nearly 10 orders of magnitude.[23] Normally in serum and plasma, the top 14 most abundant proteins comprise roughly 95% of the total protein content.[18] Previous reports that quantitatively compared suction blister-derived ISF (SBF) to serum and plasma showed that there was a significant reduction of these proteins by volume, comprising roughly 30% of the total content.[16,24] This observation was attributed to an overall higher water content that occurred during the blister generation.

## Dermal ISF Proteome versus Plasma and Serum

Thorough qualitative and quantitative evaluation of the dermal ISF proteome in comparison with patient matched plasma and serum is necessary to assess the applicability of microneedle-derived ISF as a novel minimally invasive sampling technique for clinical diagnosis and monitoring. Our analysis resulted in the identification of 3527 proteins belonging to 1244 protein groups that shared the same set or subset of identified peptides. The Venn diagram in Figure 2A shows 3270 out of the 3506 proteins identified in donor #1, equivalent to 93%, were ultimately found in common between all biological fluids. Additionally, there was very high overall proteome overlap between all three donors, as depicted in Figure 2B. Similar results were observed for donors #2 and #3 with 95% and 98% proteins in common, respectively (Figure S-1).

Relative quantification was performed for the 407 unambiguous proteins, which were identified with at least one peptide unique to the protein. Principal component analysis (PCA) showed that the global expression of the proteins identified in ISF were clearly distinguished from the serum and plasma (Figure 3A). Z-score based hierarchical classification of the samples and related proteins by the similarity in expression supported the PCA result with the fact that the ISF samples were associated in a group that is clearly distinct from the groups of plasma and serum (Figure 3B). In particular, one cluster of 113 proteins shown in orange of Figure 3B was more highly expressed in ISF, and another group of 80 proteins in pink were in lower expression.

The volcano plot in Figure 4A demonstrates high variance in quantitation between ISF and serum based on a paired Student's *t* test of the 407 quantified proteins. Of these proteins, 109 were found to be significantly different with 91 proteins changing 2-fold or higher (76 up and 15 down). Expression ratio of the changed proteins is listed in Table S-1. Statistical comparison of protein expression between ISF and plasma was also performed and depicted in Figure 4B. Similar to the ISF and serum comparison, we discovered that 104 proteins were quantitatively different between ISF and plasma, with 85 proteins that changed 2-fold or higher (65 up and 20 down). The name and expression ratio of these proteins are presented in Table S-2. We then compared the proteins found to be quantitatively distinct (±2-fold) in ISF versus plasma and serum to determine the level of conservation. As shown in Figure 5, roughly 78% or 77 protein identifications overlapped during this analysis, demonstrating the high similarity between



DOI: 10.1021/acs.jproteome.7b00642
J. Proteome Res. 2018, 17, 479−485

the three fluid types. Gene annotation enrichment analysis of this overlap showed that an overwhelming percentage (~80%) belongs to the extracellular exosome. A small percentage of proteins were found to be involved in cell-to-cell adhesion processes via binding to cadherins.

In addition to the paired Student's *t* test, an analysis of variance (ANOVA) was performed on the 407 quantified proteins across all three donors. This analysis resulted in 26 proteins that were found to be differentially expressed consistently across all three donors (Table 1).

We observed that 22 proteins were more abundant in ISF, whereas 4 other proteins were less in comparison with plasma and serum. Quantitation ISF/plasma and ISF/serum ratios of these proteins were conserved across all human donors investigated. Expression levels of the proteins were greatly diverse, as much 20 times higher for carbonyl reductase and ribonuclease inhibitor in ISF, whereas von Willebrand factor was 10 times lower. In agreement with the *t*-test evaluation, gene annotation enrichment analysis showed 19 out of the 26 proteins were in extracellular exosome (Table S-3). With an exception of protein von Willebrand factor, which was less abundant in ISF, the 18 other exosomal proteins were more highly expressed in ISF.

## CONCLUSIONS

ISF fluid was thoroughly characterized using a quantitative shotgun proteomics approach and compared with donor-matched plasma and serum. This analysis demonstrated that ISF across all three donors is highly homogeneous and nearly indistinguishable in terms of protein diversity compared with serum and plasma. Most differences were seen at the quantitative level, as the quantity of the top proteins found in ISF differed from those in serum and plasma. Statistical analysis suggests that ISF is significantly enriched with exosomes compared with serum and plasma. It should be noted that a sample size of only three subjects makes it difficult to reach statistically significant conclusions, our results still highlight proteomic trends among the three types of fluid and can be applied to much larger sample sizes in future studies. Overall, this work suggests that ISF is a minimally invasive alternative to serum and plasma, which proves useful for many clinical applications including physiological monitoring and diagnostics. The microneedle array used in this study can be further matured and serve as the sampling foundation for the development of new real-time wearable sensing technologies.

## ASSOCIATED CONTENT

### Supporting Information

The Supporting Information is available free of charge on the ACS Publications website at DOI: 10.1021/acs.jproteome.7b00642.

Figure S-1: Venn diagrams comparing total ISF proteome from three healthy donors. Table S-1: List of proteins *t* test significantly different in expression between ISF and serum. Table S-2: List of proteins *t* test significantly different in expression between ISF and plasma. Table S-3: Functional annotation analysis using DAVID of 26 ANOVA significant proteins unique to ISF. (PDF)

## AUTHOR INFORMATION


### Corresponding Authors

*T.G.: trevor.g.glaros.civ@mail.mil.
*R.P.: RPolsky@sandia.gov.

### ORCID

Trevor Glaros: 0000-0001-9922-6330

### Author Contributions

⊥B.Q.T. and P.R.M. contributed equally.


### Notes

The authors declare no competing financial interest.

## ACKNOWLEDGMENTS

We thank Parwana Ebrahimi (University of New Mexico, Department of Biomedical Engineering) for her assistance in preparing Figure 1. This research was made possible by funding provided by the Edgewood Chemical Biological Center (ECBC) through the 2017 IDEAs program and support from the Defense Threat Reduction Agency–Joint Science and Technology Office for Chemical and Biological Defense: Project 189920 to Sandia National Laboratory and CB10434 to ECBC. Conclusions and opinions presented here are those of the authors and are not the official policy of the U.S. Army, ECBC, or the U.S. Government. J.T.B. and R.M.T. received infrastructure support from NIH CTSC Grant Number: UL1TR00449. Information in this report is cleared for public release and distribution is unlimited.

## REFERENCES


(1) Mogensen, M.; Jemec, G. B. Diagnosis of nonmelanoma skin cancer/keratinocyte carcinoma: a review of diagnostic accuracy of nonmelanoma skin cancer diagnostic tests and technologies. *Dermatol. Surg.* **2007**, *33* (10), 1158–1174.

(2) Carley, S. D.; Libetta, C.; Flavin, B.; Butler, J.; Tong, N.; Sammy, I. An open prospective randomised trial to reduce the pain of blood glucose testing: ear versus thumb. *Bmj* **2000**, *321* (7252), 20.

(3) Caduff, A.; Hirt, E.; Feldman, Y.; Ali, Z.; Heinemann, L. First human experiments with a novel non-invasive, non-optical continuous glucose monitoring system. *Biosens. Bioelectron.* **2003**, *19* (3), 209–217.

(4) Wang, P. M.; Cornwell, M.; Prausnitz, M. R. Minimally invasive extraction of dermal interstitial fluid for glucose monitoring using microneedles. *Diabetes Technol. Ther.* **2005**, *7* (1), 131–141.

(5) Stern, R. C. The diagnosis of cystic fibrosis. *N. Engl. J. Med.* **1997**, *336* (7), 487–491.

(6) Donnelly, R. F.; Mooney, K.; Caffarel-Salvador, E.; Torrisi, B. M.; Eltayib, E.; McElnay, J. C. Microneedle-mediated minimally invasive patient monitoring. *Ther. Drug Monit.* **2014**, *36* (1), 1.

(7) Guy, R. Diagnostic devices: Managing diabetes through the skin. *Nat. Nanotechnol.* **2016**, *11* (6), 493–494.

(8) El-Laboudi, A.; Oliver, N. S.; Cass, A.; Johnston, D. Use of microneedle array devices for continuous glucose monitoring: a review. *Diabetes Technol. Ther.* **2013**, *15* (1), 101–115.

(9) Ng, K. W.; Lau, W. M.; Williams, A. C. Towards pain-free diagnosis of skin diseases through multiplexed microneedles: biomarker extraction and detection using a highly sensitive blotting method. *Drug Delivery Transl. Res.* **2015**, *5* (4), 387–396.

(10) Miller, P. R.; Narayan, R. J.; Polsky, R. Microneedle-based sensors for medical diagnosis. *J. Mater. Chem. B* **2016**, *4* (8), 1379–1383.

(11) Romanyuk, A. V.; Zvezdin, V. N.; Samant, P.; Grenader, M. I.; Zemlyanova, M.; Prausnitz, M. R. Collection of analytes from microneedle patches. *Anal. Chem.* **2014**, *86* (21), 10520–10523.

(12) Muller, D. A.; Corrie, S. R.; Coffey, J.; Young, P. R.; Kendall, M. A. Surface modified microprojection arrays for the selective extraction




DOI: 10.1021/acs.jproteome.7b00642
*J. Proteome Res.* 2018, 17, 479–485

of the dengue virus NS1 protein as a marker for disease. *Anal. Chem.* **2012**, *84* (7), 3262−3268.
(13) Caffarel-Salvador, E.; Brady, A. J.; Eltayib, E.; Meng, T.; Alonso-Vicente, A.; Gonzalez-Vazquez, P.; Torrisi, B. M.; Vicente-Perez, E. M.; Mooney, K.; Jones, D. S.; et al. Hydrogel-forming microneedle arrays allow detection of drugs and glucose in vivo: potential for use in diagnosis and therapeutic drug monitoring. *PLoS One* **2015**, *10* (12), e0145644.
(14) Cengiz, E.; Tamborlane, W. V. A tale of two compartments: interstitial versus blood glucose monitoring. *Diabetes Technol. Ther.* **2009**, *11* (S1), S-11−S-16.
(15) Moulder, R.; Bhosale, S. D.; Goodlett, D. R.; Lahesmaa, R. Analysis of the plasma proteome using iTRAQ and TMT-based Isobaric labeling. *Mass Spectrom. Rev.* **2017**, DOI: 10.1002/mas.21550.
(16) Müller, A. C.; Breitwieser, F. P.; Fischer, H.; Schuster, C.; Brandt, O.; Colinge, J.; Superti-Furga, G.; Stingl, G.; Elbe-Bürger, A.; Bennett, K. L. A comparative proteomic study of human skin suction blister fluid from healthy individuals using immunodepletion and iTRAQ labeling. *J. Proteome Res.* **2012**, *11* (7), 3715−3727.
(17) Gilar, M.; Olivova, P.; Daly, A. E.; Gebler, J. C. Orthogonality of separation in two-dimensional liquid chromatography. *Anal. Chem.* **2005**, *77* (19), 6426−6434.
(18) Keshishian, H.; Burgess, M. W.; Gillette, M. A.; Mertins, P.; Clauser, K. R.; Mani, D.; Kuhn, E. W.; Farrell, L. A.; Gerszten, R. E.; Carr, S. A. Multiplexed, quantitative workflow for sensitive biomarker discovery in plasma yields novel candidates for early myocardial injury. *Mol. Cell. Proteomics* **2015**, *14*, 2375.
(19) Käll, L.; Canterbury, J. D.; Weston, J.; Noble, W. S.; MacCoss, M. J. Semi-supervised learning for peptide identification from shotgun proteomics datasets. *Nat. Methods* **2007**, *4* (11), 923−925.
(20) Cox, J.; Mann, M. 1D and 2D annotation enrichment: a statistical method integrating quantitative proteomics with complementary high-throughput data. *BMC Bioinf.* **2012**, *13* (16), S12.
(21) Dennis, G.; Sherman, B. T.; Hosack, D. A.; Yang, J.; Gao, W.; Lane, H. C.; Lempicki, R. A. DAVID: database for annotation, visualization, and integrated discovery. *Genome Biol.* **2003**, *4* (9), R60.
(22) Kool, J.; Reubsaet, L.; Wesseldijk, F.; Maravilha, R. T.; Pinkse, M. W.; D'Santos, C. S.; van Hilten, J. J.; Zijlstra, F. J.; Heck, A. J. Suction blister fluid as potential body fluid for biomarker proteins. *Proteomics* **2007**, *7* (20), 3638−3650.
(23) Righetti, P. G.; Castagna, A.; Antonucci, F.; Piubelli, C.; Cecconi, D.; Campostrini, N.; Rustichelli, C.; Antonioli, P.; Zanusso, G.; Monaco, S.; et al. Proteome analysis in the clinical chemistry laboratory: myth or reality? *Clin. Chim. Acta* **2005**, *357* (2), 123−139.
(24) Svedman, C.; Yu, B. B.; Ryan, T. J.; Svensson, H. Plasma proteins in a standardised skin mini-erosion (II): effects of extraction pressure. *BMC Dermatol.* **2002**, *2* (1), 4.



DOI: 10.1021/acs.jproteome.7b00642
*J. Proteome Res.* 2018, 17, 479−485